

Optimization of Nanopatterned Multilayer Hyperbolic Metamaterials for Spontaneous Light Emission Enhancement

Dylan Lu, Lorenzo Ferrari, Jimmy J. Kan, Eric E. Fullerton, and Zhaowei Liu*

Light emission processes can be modified through the Purcell effect near a metallic surface. Such effect relies on the matching between spontaneous emission spectra and surface plasmon resonances, and the latter is typically limited by the existing metal properties. Nanopatterned multilayer hyperbolic metamaterials (HMMs) with engineerable material property are promising in enhancing spontaneous emission rates at desired frequencies with improved far-field radiative power. In this work, the authors study the optimization process for spontaneous emission enhancement by using nanopatterned HMMs. By theoretically investigating the Purcell effect on HMMs compared with traditional metals, the authors choose better material combinations for stronger Purcell enhancement. Different decay channels in the HMM are analyzed against the emitter distance and their wavelengths. Systematic optimization of achieving large emission intensity is demonstrated by comparing performance of nanopatterned HMMs with different geometry parameters. The promise in achieving light emission with both high decay rates and brightness has various potential applications including light-emitting devices, single-molecule detection, and surface-enhanced Raman scattering.

devices,^[4] as well as in light detection, such as biosensing and surface-enhanced Raman scattering,^[5] and may also impact DNA targeting in genome sequencing.^[6] Spontaneous emission is strongly modified when light emitters interact with their local electromagnetic environment, which alters the relative contribution of different energy releasing routes or decay channels. As opposed to the case of cavities with high Q-factor,^[7] light emission near metal surfaces excites surface plasmon resonances with strong electric field enhancement, which introduces a dominating decay channel due to the high photonic density of states (PDOS) in surface plasmons.^[2–4] In order to enhance decay rates, the emission wavelengths must be aligned with plasmonic resonances which are determined by the intrinsic material properties of a metal. Therefore, such an approach only works for a few narrow bands of frequencies due to the limited available plasmonic materials existing in nature.

1. Introduction

The process of light emission from quantum sources and its control through the Purcell effect has been widely explored in recent years.^[1–3] This phenomenon has a number of potential applications in light generation, such as solid-state lighting

In contrast with conventional metallic materials, metamaterials offer new solutions to design material properties with potential applications in super-resolution imaging, and tunable multifunctional devices.^[8] Hyperbolic metamaterials (HMMs) with unbounded isofrequency surface support plasmonic modes with high wavevectors, and have recently attracted significant attention for their extraordinary optical properties.^[9–11] When brought within the near field of a HMM, light emitters decay to the lower-energy level by releasing energy mainly through three channels: radiative emission, HMM plasmonic modes, and other non-radiative decay modes usually referred as lossy wave components.^[2,12] Plasmonic modes spreading over a wide range of wavevectors in HMMs dominate over other channels. Therefore, they provide a large PDOS in the wavelength range where hyperbolic dispersions are achieved, yielding a concomitant strong enhancement in emission rates. More remarkably, this enhancement is broadband and also tunable by simply changing the filling ratio of the constituent materials.

Multilayer-based HMMs have been utilized to control light emission process, however, only a moderate Purcell enhancement has been observed using uniform multilayer films.^[11–13] It is not only due to difficulties in fabricating metal-dielectric multilayers with deep subwavelength periods but also because

Dr. D. Lu, Prof. E. E. Fullerton, Prof. Z. Liu
Department of Electrical and Computer Engineering
University of California
San Diego, 9500 Gilman Drive, La Jolla, CA 92093-0407, USA
E-mail: zhaowei@ucsd.edu

Dr. L. Ferrari, Prof. Z. Liu
Materials Science and Engineering
University of California
San Diego, 9500 Gilman Drive, La Jolla, CA 92093-0418, USA

Dr. J. J. Kan, Prof. E. E. Fullerton, Prof. Z. Liu
Center for Memory and Recording Research
University of California
San Diego, 9500 Gilman Drive, La Jolla, CA 92093-0401, USA

 The ORCID identification number(s) for the author(s) of this article can be found under <https://doi.org/10.1002/pssa.201800263>.

DOI: 10.1002/pssa.201800263

the dominating HMM plasmonic modes in uniform multilayer metamaterials are normally non-radiative. As a consequence, radiative emission efficiency for light emitters on uniform multilayers becomes diminished, which prevents the detection of large Purcell enhancement in the far field. The incorporation of out-coupling nanostructures into HMMs provides an effective platform to engineer PDOS and radiative emission simultaneously as have been demonstrated recently.^[14–16]

In this work, we optimize nanopatterned multilayer HMMs for enhancing light emission by theoretical modeling and numerical simulation. Both strongly enhanced decay rates and improved radiative emission into the far field have been achieved by better choice of material combination and optimized design of multilayer and nanopattern geometry. Through the study of Purcell effect on flat pure metallic films and uniform metal-dielectric multilayer HMMs, we identify the choice of metallic materials and the material combination and configurations in the multilayers. Different decay channels that contribute to the Purcell enhancement are also compared and analyzed. The HMM plasmonic modes have a major contribution to the emission decay and therefore should be fully utilized for efficient outcoupling. We provide the guideline for such plasmonic substrate design by comparing intensity enhancement performance of nanopatterned HMMs with different grating periods.

2. Results and Discussion

To characterize the interaction between dipole light emitters and plasmonic substrate, we use the theoretical framework^[14] to calculate such quantities as Purcell factor F , radiative enhancement f_{rad} , and external quantum efficiency (EQE) enhancement f_n for dipole emitters on top of metal films and multilayer HMM substrates as shown in **Figure 1**. The study of nanopatterned multilayer HMM is carried out by three-dimensional (3D) full-wave electromagnetic simulations.^[14] The ultimate emission intensity enhancement is governed by both the radiative enhancement and the absorption enhancement, $f_F = f_{\text{rad}} \cdot |E/E_0|^{2N}$, where E and E_0 are the electric field at the excitation wavelength applied on the dipole emitter near the substrate and in free space, respectively. $N = 1$ and 2 for single-photon excitation and two-photon excitation processes, respectively. The absorption enhancement will be obtained by separate calculations that evaluates electrical field enhancement when a plane wave is incident onto the plasmonic

substrates as compared with in free space at the excitation wavelength.

Figure 2 shows the calculated Purcell factors and the corresponding dispersion relations for conventional plasmonic metallic materials, Ag, Al, and Au. The permittivity for Ag is taken from ref. [17] while those for Al and Au from ref. [18]. The surrounding medium is assumed to have $\epsilon_1 = 2.25$. In the calculations of Purcell factor, the dipole emitter is surrounded by a dielectric medium of the same permittivity $\epsilon_1 = 2.25$ and placed $d = 10$ nm above a 200 nm thick metal on a glass substrate. Purcell factors for isotropic dipoles are obtained by averaging over the results of dipoles parallel and perpendicular to the surface.

For pure metallic substrates, the decay rate is enhanced when the emission wavelength aligns with the surface plasmon resonance. Corresponding high PDOS at these surface plasmon resonances leads to strong Purcell effect. Owing to its superior plasmonic property extended to higher wavevectors, Ag shows a decay rate enhancement of two orders of magnitude at the resonance $\lambda = 360$ nm, which is much higher than other commonly available plasmonic metals in the optical wavelength. The plasmonic resonance frequency is determined by the permittivities of both metal and the dielectric, which is limited by the properties of existing materials. For dipole emissions at wavelengths not aligned with the resonances, the Purcell enhancement by these conventional plasmonic materials diminishes.

As compared with the fixed plasmonic resonances in metals, multilayer-based metamaterials provide the solution for tunable material properties not available in nature. Owing to the superior performance, Ag is chosen as the metal component. **Figure 3a** shows the Purcell factors calculated for isotropic dipole emitters in a dielectric medium with $\epsilon_1 = 2.25$ at a distance $d = 10$ nm away from uniform Ag-Si HMMs. The multilayer metamaterial consists of 10 layers of Ag and 11 layers of Si with a period of 20 nm on a glass substrate. The permittivity for Si is taken from ref. [19]. The filling ratio p of Ag varies from 1 to 0.4 with $p = 1$ corresponding to a pure Ag film.

By varying the constituent material filling ratio, Purcell enhancement peak of Ag-Si HMMs can be tuned across the visible spectrum with a broader bandwidth in contrast with a fixed one by pure Ag film at $\lambda = 360$ nm with a narrow bandwidth of about 10 nm. The tunability in multilayer metamaterials demonstrates engineered material properties and enables

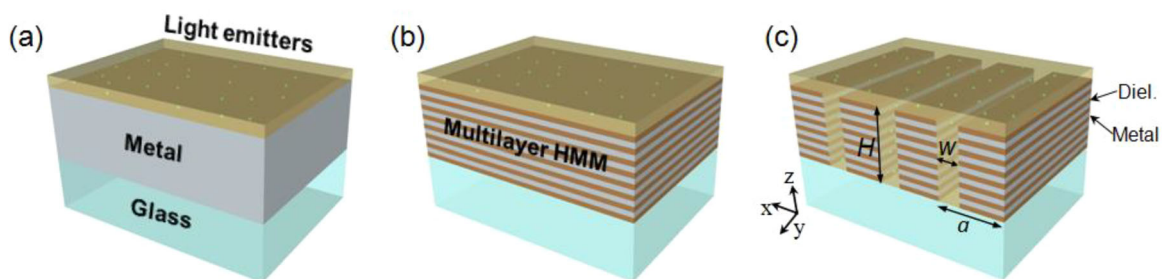


Figure 1. Schematics of the light emitter-substrate interaction systems: light emitters embedded in a dielectric medium with a permittivity ϵ_1 locate in the vicinity of (a) a metal film, (b) a uniform multilayer HMM, and (c) a nanopatterned multilayer HMM. All the structures are assumed to be on top of glass substrates. The nanopatterned HMM has period a , nanoslit width w , and height H .

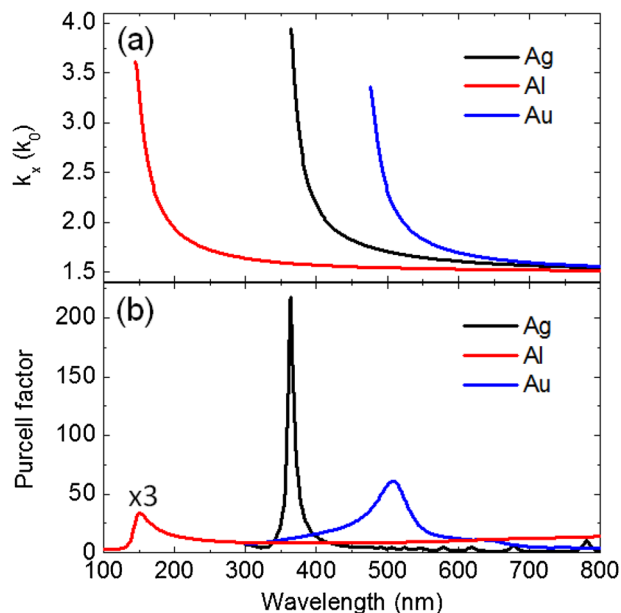


Figure 2. a) Dispersion relations for electromagnetic waves at the interfaces between metals, Ag (black), Al (red), and Au (blue), and a dielectric medium with permittivity $\epsilon_1 = 2.25$. b) Purcell factor calculated for isotropic dipole emitters located a distance of $d = 10$ nm above a 200 nm thick metal of Ag (black), Al (red), and Au (blue) on a glass substrate with a permittivity of 2.25. The magnitude of Purcell factor for Al is multiplied by 3 for better comparison.

optimized alignment of Purcell effect with different emission spectra from molecules or semiconductors. For instance, the decay rate around the wavelength of 580 nm will be enhanced by close to 120-fold for the HMMs with $p = 0.6$ but less than fivefold

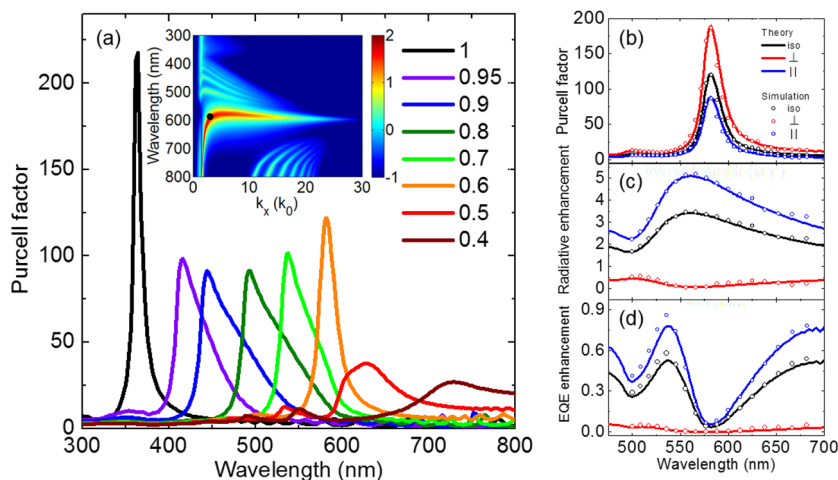


Figure 3. a) Purcell factor for isotropic dipole emitters located at a distance $d = 10$ nm away from the top surface of uniform Ag-Si HMMs. The multilayers consist of 10 layers of Ag and 11 layers of Si with a period of 20 nm on a glass substrate with a permittivity of 2.25. The filling ratio of Ag varies from 1 to 0.4 as indicated by different colors. The inset shows the normalized dissipated power spectrum with the intensity on a logarithmic scale for a dipole perpendicular to the HMM with a Ag filling ratio of 0.6. The black dot corresponds to the inverse grating period of 200 nm. b) Purcell factor, (c) radiative enhancement, and (d) EQE enhancement for dipoles of the isotropic orientation (iso, black lines), perpendicular (\perp , red lines), and parallel (\parallel , blue lines) to the uniform HMM surface in the case of a Ag filling ratio of 0.6. The results of corresponding 3D full-wave simulations in open circles agree with the theoretical calculations.

for pure Ag whose surface plasmon resonance is far away from the emission wavelength.

At the wavelength of peak Purcell enhancement, dipole emissions on multilayer metamaterials are strongly modified because the extraordinary hyperbolic dispersions in HMMs creates additional high wave-vector modes, leading to increased PDOS at the resonance wavelengths for the spontaneous decay.^[9,12] The inset of Figure 3a shows the normalized dissipated power spectrum for a perpendicular dipole above a HMM with $p = 0.6$. It represents different decay channels, showing the high wave-vector modes in the HMM at the resonance wavelength $\lambda = 582$ nm.

In the calculation for multilayers, the first layer interacting with the dipole emitter is set to be Si. Therefore, the peak magnitude of the Purcell factor in HMMs is lower than that in pure Ag, and further drops at smaller metallic filling ratio as the effective distance between emitters and first Ag layer is enlarged. However, it can be increased to the level of pure Ag by shrinking the thickness of the first layer.

To further understand the Purcell effect in HMMs, we inspect the Ag-Si HMM with a Ag filling ratio of 0.6 in Figure 3b–d. Figure 3b shows analytical calculations of Purcell factor for dipoles perpendicular and parallel to the multilayer surface whose average gives the result for isotropic dipoles. Perpendicular dipoles have stronger Purcell enhancement than parallel dipoles due to the constructive interference of electric field in the near field of the substrate.^[3] On average, a decay-rate enhancement of close to 120-fold is achievable for isotropic dipoles at the wavelength $\lambda = 582$ nm. Such a high Purcell enhancement consists of mainly three contributions including radiative emission, HMM plasmonic modes, and lossy waves. The latter two components are non-radiative in uniform HMMs

whereas radiative emission can be collected within a corresponding observation angle in the far field. Figure 3c depicts the radiative enhancement which reaches maximum almost at the same wavelength as the Purcell factor for isotropic dipoles. However, the EQE enhancement becomes accordingly a minimum as shown in Figure 3d since radiative enhancement is still a small portion of the Purcell factor. This may prevent the observation of strong Purcell effect in the far field and limit practical applications of such Purcell enhancement. All these analytical results are also well reproduced by those from full-wave simulations as shown in Figure 3 in open circles, which confirms the validity of numerical simulations.

To better engineer the radiative emission, a detailed analysis of the contribution from different decay channels will be helpful as shown in Figure 4. The distribution of different decay channels depends on both the emission wavelength and the emitter-metamaterial distance. Figure 4a–c show the spectra of radiative emission, HMM plasmonic modes and lossy-wave components

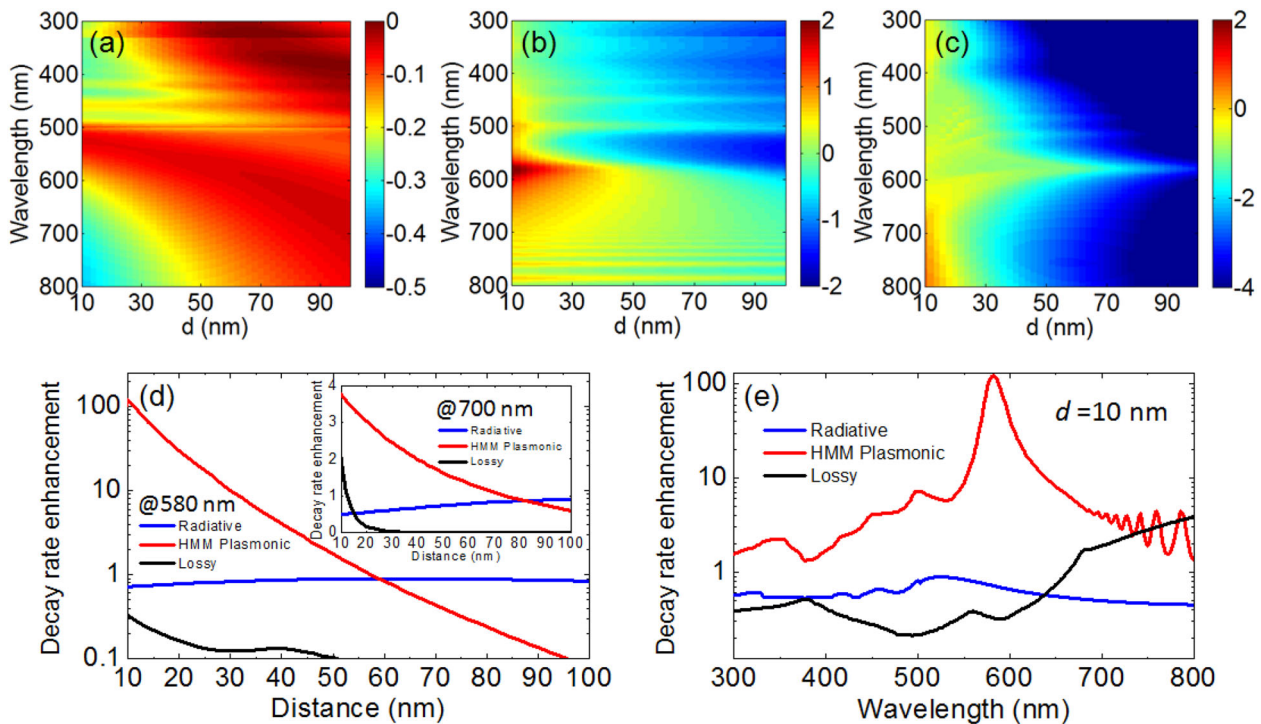


Figure 4. a) Radiative emission, (b) HMM plasmonic modes, and (c) lossy-wave component spectra plotted with the intensity on a logarithmic scale for dipole emitters of isotropic orientation located at a distance of d varying from 10 to 100 nm away from the top surface of uniform Ag-Si HMM. The multilayers consist of 10 layers of Ag and 11 layers of Si with a period of 20 nm on a glass substrate with a permittivity of 2.25. The filling ratio of Ag is 0.6. d) Three channels of decay rate enhancement as a function of the emitter-metamaterial distance d at the wavelength $\lambda = 582$ nm based on (a–c). The inset shows the same quantities at $\lambda = 700$ nm. e) Three channels of decay rate enhancement as a function of the emission wavelength at a fixed distance $d = 10$ nm.

as the emitter-metamaterial distance increases from 10 to 100 nm. The radiative emission is obtained by the integration of normalized dissipated power over the wave-vector range of $0 < k_x < \sqrt{\epsilon_1} k_0$. The contribution of the HMM plasmonic modes is calculated by integrating normalized dissipated power near the plasmonic resonances, whereas the rest of power dissipation at high wavevector will be due to lossy waves.^[2] The results indicate that radiative emission from emitters close to the uniform HMM contributes a small portion of the Purcell effect and barely depends on the distance and the wavelength (Figure 4d,e). Most of the dissipated power goes to HMM plasmonic modes and lossy-wave component, which are non-radiative in uniform HMM. Since lossy-wave component corresponds to very high wave-vector modes which are inefficiently coupled out and ultimately lost as heat, HMM plasmonic modes represent the portion that will potentially contribute to far-field emission. Such plasmonic enhancement is exponentially decaying away, mostly confined in space within the short distance of 10–30 nm from the HMM surface (Figure 4b,d), and is concentrated close to the resonance wavelength $\lambda = 582$ nm (Figure 4b,e). In order to extract this contribution into the far field for enhanced radiative emission, an out-coupling mechanism is needed to compensate for the wave-vector mismatch between HMM plasmonic modes and propagating modes in free space.

In order to effectively turn the plasmonic component of Purcell enhancement into radiative enhancement, we

implement a one-dimensional grating nanostructure in the HMM and illustrate the optimization process by sweeping the grating period in **Figure 5**. Based on the 3D full-wave simulations, spatial distributions of Purcell factor, radiative enhancement and emission intensity enhancement are mapped out at the emission wavelength 582 nm. The sweeping step length is 10 nm, and the dipole is kept at least 10 nm away from the surface of the HMM. The integration angle for radiative power limits the collected wavevectors within the cutoff wavevector $k_{cf} = 0.75k_0$. Purcell factor maintains its maximum at a distance of 10 nm away from the HMM surface for different periods, with a slightly smaller enhancement when the grating period is 80 nm (Figure 5a,d), whereas the radiative enhancement transits from resonances with one node to those with two nodes until off resonance as the period increases. A largest enhancement of radiative emission was found at a grating period 200 nm. The inverse grating period corresponds to the black dot in the inset of Figure 3a, which matches the plasmonic resonance wavevectors for most efficient out-coupling. The non-radiative plasmonic modes in the nanopatterned HMM will then propagate to the far field. The averaged radiative enhancement over all the spatial locations assuming a uniform emitter distribution also indicates a maximum of over sixfold enhancement at a period 200 nm as the red line shown in Figure 5d. The ultimate emission intensity enhancement directly measurable in a photoluminescence system will be also determined by the absorption enhancement as predicted in Figure 5c. In this

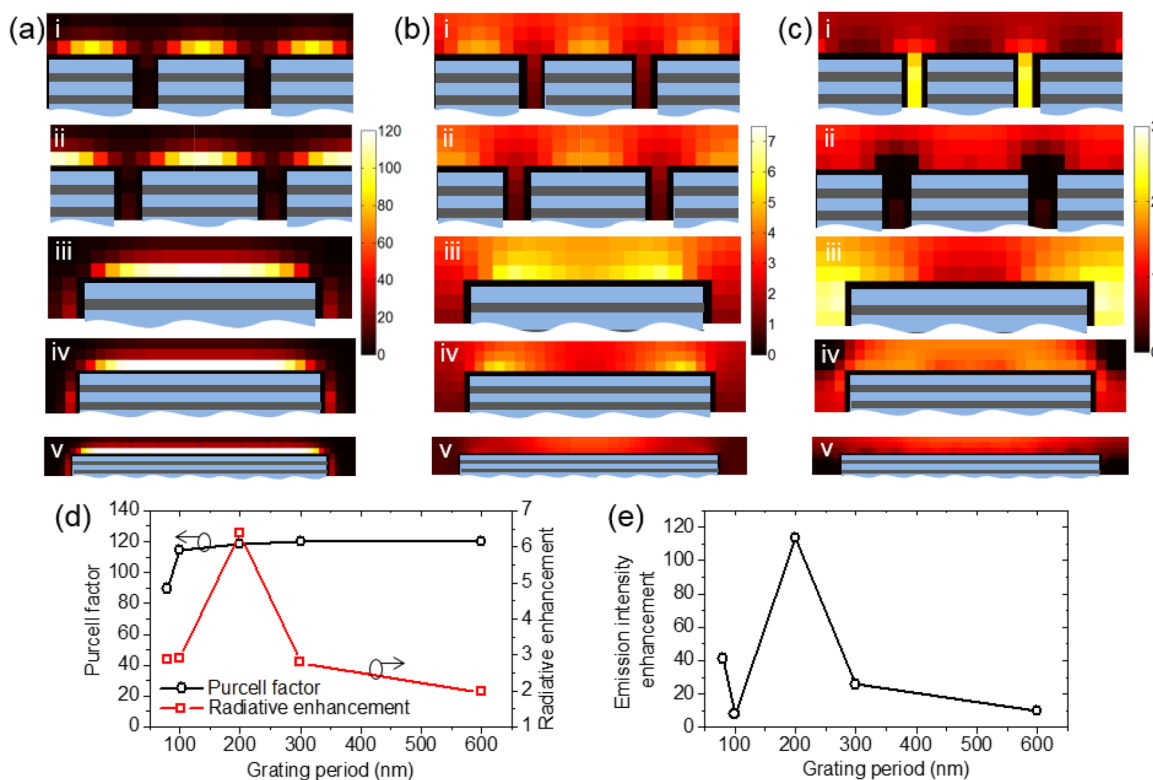


Figure 5. Spatial distribution of (a) Purcell factor, (b) radiative enhancement, and (c) emission intensity enhancement for a single dipole emitter of isotropic orientation above nanopatterned Ag-Si HMMs with different grating periods at the emission wavelength $\lambda = 582$ nm. The periods are i) 80 nm, ii) 100 nm, iii) 200 nm, iv) 300 nm, and v) 600 nm, respectively, with a fixed duty cycle 0.8. The multilayers consist of 10 layers of Ag and 11 layers of Si with a period of 20 nm on a glass substrate with a permittivity of 2.25. The filling ratio of Ag is 0.6. The spatial mapping step size is 10 nm. Plots for iv) and v) are not on the same scale as the rest. Magnitude for the emission intensity enhancement (c) is on a logarithmic scale. The two-photon excitation wavelength is 730 nm. d) Purcell factor (black) and radiative enhancement (red) as a function of the grating period. Purcell factor is for the emitter at the middle location of HMM. Radiative enhancement is averaged among all the spatial locations. e) Emission intensity enhancement as a function of the grating period averaged among all the spatial locations.

specific example, a two-photon excitation process was chosen at a wavelength of 730 nm. The local emission intensity at a specific spatial position can be enhanced >1000 -fold when the grating period is 200 nm although the averaged emission intensity enhancement among all dipole locations is about 120-fold (Figure 5e). The dependence of average emission intensity enhancement on the grating period shows similar trend as the average radiative enhancement in this case. A different excitation process or excitation wavelength may end up a different trend in the emission intensity enhancement. Therefore, optimization of the emission intensity enhancement needs a systematic design that takes both excitation and emission processes into account.

Based on the optimized nanopatterned Ag-Si HMMs with a trench period $a = 200$ nm and width $w = 40$ nm, Figure 6 further show the spectral dependence of Purcell factor and radiative enhancement. At dipole locations of 1 and 2 (Figure 6a), Purcell factor as a function of the emission wavelengths in Figure 6c confirms the spectral similarity between uniform and nanopatterned HMM. In addition, the Purcell enhancement close to the sidewall of the nanoslit at location three shifts to longer wavelengths because of the anisotropic material property of multilayer-based metamaterials and coupling between HMM nanoridges. On the other hand, radiative emission is

significantly enhanced in nanopatterned HMMs thanks to the out-coupling effect of the grating as shown in Figure 6a,d. It has more improvement closer to the surface of the HMM where higher PDOS is available for out-coupling. Compared with light emitters in free space, radiative emission on nanopatterned HMM at locations 1' and 2' gets enhanced by over sixfold around the peak Purcell enhancement at 582 nm, which is $\approx 100\%$ improvement over uniform HMM. The radiative emission enhancement also leads to the same increase in the EQE. Compared with 1' and 2', radiative enhancement at 3' is low around the wavelength 582 nm but shifts to longer wavelength. It is noted that the misalignment between peak Purcell and radiative enhancement is larger at 3' than 1' and 2', indicating emitter locations on top of the HMM is preferred for achieving both decay rate and radiative emission enhancement. The mechanism of such improvement can be further understood by comparing the angular distribution of radiative enhancement on different substrates as given in Figure 6b. Light emission on the nanopatterned HMM has a stronger radiative intensity and better directionality into the observation angle than on the uniform HMM by outcoupling the HMM plasmonic modes. The radiative enhancement on the nanopatterned HMM is a combined effect of both plasmonic outcoupling and the

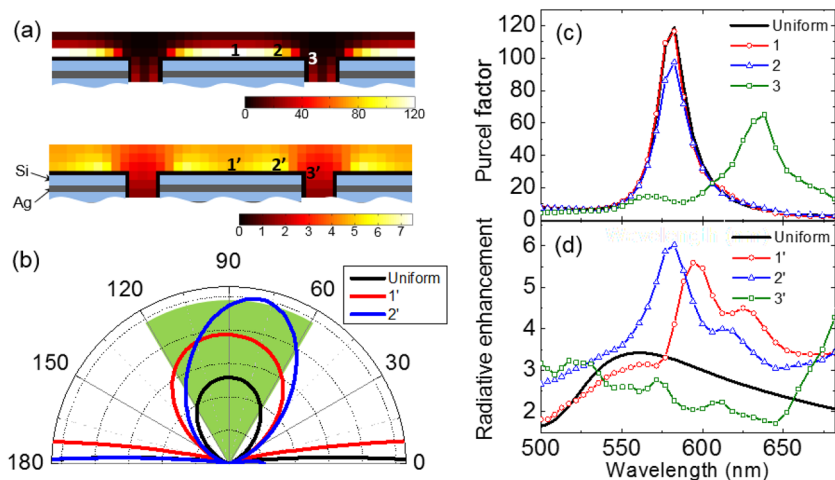


Figure 6. a) Spatial distribution of Purcell factor (up) and radiative enhancement (down) for a single dipole emitter of isotropic orientation swept across different positions above nanopatterned Ag-Si HMMs at the wavelength $\lambda = 582$ nm. The multilayers consist of 10 layers of Ag and 11 layers of Si with a period of 20 nm on a glass substrate with a permittivity of 2.25. The filling ratio of Ag is 0.6. The nanoslits have a period 200 nm and a width 40 nm. b) Angular distribution of radiative enhancement in the x-z plane for a single dipole emitter oriented along x axis above uniform and nanopatterned Ag-Si HMMs at the locations indicated in (a). The emission wavelength for the uniform HMM and locations 2' is chosen at $\lambda = 582$ nm. The emission wavelength $\lambda = 594$ nm for location 1'. The green region indicates the collection angles. c) Purcell factor and (d) radiative enhancement as a function of the emission wavelength at the uniform HMM and locations indicated in (a).

collection efficiency. Designs that optimize the geometry of the grating should provide a promising solution for light emission with both enhanced decay rates and strong radiative emission.

In the calculations, the distance between dipole emitters and substrates is kept larger than 10 nm. In the regime of smaller distances, the classical theoretical model may overestimate the dipole-substrate interaction, and a nonlocal or quantum description of the interaction process has to be adopted.^[2] At a distance of a few nanometers, Purcell factor will be dramatically enhanced up to a couple of thousands. However, most of dissipated power would be channeled into lossy waves or other non-radiative decay routes which are inefficiently coupled out. Such high Purcell enhancement would lead only to a diminished EQE without benefiting far-field radiative emission. Therefore, we focus exclusively on the classical regime where plasmonic modes dominate.

Our results indicate that at the wavelength of peak Purcell enhancement the EQE for dipole emitters on the metamaterial substrate is always smaller than that in free space since the intrinsic internal quantum efficiency of the emitters is assumed to be unity. A large EQE enhancement is possible only when the internal quantum efficiency of quantum emitters is low. However, low internal quantum efficiency would cause a concomitant drop in the Purcell factor. Therefore, in order to utilize the Purcell effect, quantum emitters with high quantum efficiency are needed. Despite of low EQE enhancement, radiative emission into the far field can be enhanced.

We made use of a grating nanostructured HMMs to extract plasmonic modes into the far field. The possible out-coupling structures are not limited to one-dimensional geometries, but can include for instance two-dimensional arrays.^[16] The ultimate

brightness of emitters on the HMM substrates is not only determined by the radiative enhancement but also absorption enhancement if an optical excitation is used. Hence, design procedures combining enhanced electrical field intensity at the absorption wavelength and enhanced radiation at the emission wavelength are needed. Besides, the averaged emission intensity also strongly depends on the spatial distribution of light emitters and their orientations.

3. Conclusion

In conclusion, we studied the optimization of nanopatterned HMM substrates for Purcell enhancement of spontaneous light emission. The design principle lies on the smart choice of material combination and optimized design of multilayer and nanopattern geometry. Through detailed analysis of different decay channels, HMM plasmonic modes were identified as a major component to be efficiently outcoupled to the far field. The effective outcoupling structure design was illustrated by comparing Purcell factor and emission intensity enhancement of nanopatterned HMMs with different grating periods. Light emission with both enhanced decay rates and high brightness can be obtained following the design principle, paving the way for an easy and versatile control of spontaneous emission in quantum emitters.

Acknowledgements

The authors acknowledged financial support from National Science Foundation – Division of Materials Research (grant no. 1610538), and ONR MURI program (no. N00014-13-1-0678).

Conflict of Interest

The authors declare no conflict of interest.

Keywords

metamaterials, multilayers, plasmonics, Purcell effect, spontaneous emission

Received: March 30, 2018
Revised: September 18, 2018
Published online:

[1] a) E. M. Purcell, *Phys. Rev.* **1946**, 69, 681; b) P. Anger, P. Bharadwaj, L. Novotny, *Phys. Rev. Lett.* **2006**, 96, 113002; c) K. T. Shimizu, W. K. Woo, B. R. Fisher, H. J. Eisler, M. G. Bawendi, *Phys. Rev. Lett.* **2002**, 89, 117401.

- [2] G. W. Ford, W. H. Weber, *Phys. Rep.* **1984**, *113*, 195.
- [3] W. L. Barnes, *J. Mod. Opt.* **1998**, *45*, 661.
- [4] K. Okamoto, I. Niki, A. Shvartser, Y. Narukawa, T. Mukai, A. Scherer, *Nat. Mater.* **2004**, *3*, 601.
- [5] a) H. G. Frey, S. Witt, K. Felderer, R. Guckenberger, *Phys. Rev. Lett.* **2004**, *93*, 200801; b) T. H. Taminiau, F. D. Stefani, F. B. Segerink, N. F. Van Hulst, *Nat. Photonics* **2008**, *2*, 234; c) S. M. Nie, S. R. Emery, *Science* **1997**, *275*, 1102.
- [6] M. J. Levene, J. K. S. W. Turner, M. Foquet, H. G. Craighead, W. W. Webb, *Science* **2003**, *299*, 682.
- [7] a) P. Lodahl, A. F. van Driel, I. S. Nikolaev, A. Irman, K. Overgaag, D. Vanmaekelbergh, W. L. Vos, *Nature* **2004**, *430*, 654; b) S. Noda, M. Fujita, T. Asano, *Nat. Photonics* **2007**, *1*, 449.
- [8] a) Z. Liu, H. Lee, Y. Xiong, C. Sun, X. Zhang, *Science* **2007**, *315*, 1686; b) X. Zhang, Z. Liu, *Nat. Mater.* **2008**, *7*, 435; c) N. I. Zheludev, Y. S. Kivshar, *Nat. Mater.* **2012**, *11*, 917.
- [9] D. Lu, Z. Liu, *Nat. Commun.* **2012**, *3*, 1205.
- [10] a) C. L. Cortes, W. Newman, S. Molesky, Z. Jacob, *J. Opt-Uk.* **2012**, *14*, 063001; b) Z. Jacob, V. M. Shalaev, *Science* **2011**, *334*, 463; c) Z. Jacob, I. I. Smolyaninov, E. E. Narimanov, *Appl. Phys. Lett.* **2012**, *100*, 181105; d) X. Yang, J. Yao, J. Rho, X. Yin, X. Zhang, *Nat. Photonics* **2012**, *6*, 450; e) Y. Cui, K. H. Fung, J. Xu, H. Ma, Y. Jin, S. He, N. X. Fang, *Nano Lett.* **2012**, *12*, 1443; f) H. Shen, D. Lu, B. VanSaders, J. J. Kan, H. Xu, E. E. Fullerton, Z. Liu, *Phys. Rev. X* **2015**, *5*, 021021.
- [11] H. N. S. Krishnamoorthy, Z. Jacob, E. Narimanov, I. Kretzschmar, V. M. Menon, *Science* **2012**, *336*, 205.
- [12] Z. Jacob, J.-Y. Kim, G. V. Naik, A. Boltasseva, E. E. Narimanov, V. M. Shalaev, *Appl. Phys. B* **2010**, *100*, 215.
- [13] J. Kim, V. P. Drachev, Z. Jacob, G. V. Naik, A. Boltasseva, E. E. Narimanov, V. M. Shalaev, *Opt. Exp.* **2012**, *20*, 8100.
- [14] D. Lu, J. J. Kan, E. E. Fullerton, Z. Liu, *Nat. Nanotechnol.* **2014**, *9*, 48.
- [15] L. Ferrari, D. L. Lu, D. Lepage, Z. W. Liu, *Opt. Exp.* **2014**, *22*, 4301.
- [16] D. Lu, H. Qian, K. Wang, H. Shen, F. Wei, Y. Jiang, E. E. Fullerton, P. K. L. Yu, Z. Liu, *Adv. Materials* **2018**, *30*, 1706411.
- [17] P. B. Johnson, R. W. Christy, *Phys. Rev. B* **1972**, *6*, 4370.
- [18] M. J. Weber, *Handbook of Optical Materials*. CRC Press LLC, Boca Raton **2003**.
- [19] D. E. Aspnes, A. A. Studna, *Phys. Rev. B* **1983**, *27*, 985.